Electron spin polarization in supramolecular polymers with complex pathways

Kyeong-Im Hong,[a,b,#] Abhinandan Kumar,[c#] Ana M. Garcia,[a,b,d] Subrata Majumder,[c]* Amparo Ruiz-Carretero[a,b]*

Affiliations

[a] University of Strasbourg, Institute Charles Sadron, CNRS, UPR22, 23 Rue du Loess, 67034, Strasbourg Cedex 2, France.

[b] University of Strasbourg Institute for Advanced Study, 5 allée du Général Rouvillois, F-67083 Strasbourg, France

[c] Department of Physics, National Institute of Technology, Patna 800005, India

[d] Instituto Regional de Investigación Científica Aplicada (IRICA), Universidad de Castilla-La Mancha, 13071 Ciudad Real, Spain; Faculty of Chemical Science and Technology, Universidad de Castilla-La Mancha, 13071 Ciudad Real, Spain

* Corresponding authors

#Equal contribution

E-mail: amparo.ruiz@ics-cnrs.unistra.fr, subrata@nitp.ac.in

Abstract

Mastering the manipulation of the electron spin plays a crucial role in comprehending the behavior of organic materials in various practical applications, such as asymmetric catalysis, chiroptical switches, and electronic devices. A promising avenue for achieving precise such control lies in the Chiral Induced Spin Selectivity (CISS) effect, where electrons with a favored spin exhibit preferential transport through chiral assemblies of specific handedness. Chiral supramolecular polymers emerge as excellent candidates for exploring the CISS effect due to their ability to modulate their helical structure through noncovalent interactions. Chiral supramolecular polymers capable of responding to external stimuli are

particularly intriguing, sometimes even displaying chirality inversion. This study unveils spin selectivity in chiral supramolecular polymers, derived from single enantiomers, through scanning tunneling microscopy (STM) conducted in scanning tunneling spectroscopy (STS) mode. Following two distinct sample preparation protocols for each enantiomer, we generate supramolecular polymers with opposite handedness and specific spin transport characteristics. Our primary focus centers on chiral π-conjugated building blocks, with the aim of advancing novel systems that can inspire the organic spintronics community from a supramolecular chemistry level.

Key words

Supramolecular chirality; spin polarization; CISS effect; chirality inversion

Introduction

Controlling processes occurring at the nanoscale plays a vital role in understanding the macroscopic properties of materials. An intriguing example of such control involves the manipulation of electron spin, which allows us to explain significant biological mechanisms like the migratory behavior of birds[1] or chemical transformations at the molecular level.[2] A promising approach for achieving this control is the Chiral Induced Spin Selectivity (CISS) effect.[3,4] It states that electrons with a preferred spin are transported more efficiently through chiral assemblies of specific handedness. The CISS effect was first reported in 1999 by Naaman and collaborators while studying the photoelectric effect on gold-coated slides exposed to laser light.[4] When using right-handed circularly polarized laser light, the ejected electrons were preferentially spin up, whereas they were spin down for left-handed light. When the gold-layer was covered with L-stearoyl lysine they found that spin-up electrons were transmitted more than spin-down electrons and due to symmetry, spin-down was more transmitted by D-stearoyl lysine. Interestingly, the authors concluded that it is not chirality at the molecular scale that matters, but rather a chiral arrangement of molecules. The authors showed that supramolecular chirality was needed for the CISS effect to take effect. Inspired by this pioneering work, researchers have explored various chiral

supramolecular structures in different materials, including DNA/oligopeptides,[5–11] perovskites,[12] polymers,[13,14] covalent organic frameworks[15] and in overcrowded alkenes.[16]

In particular, supramolecular polymers have emerged as promising candidates for investigating the CISS effect due to their ability to form chiral structures through noncovalent interactions.[17] Additionally, their helical structure can be reversibly modulated thanks to their noncovalent nature. Recent studies have demonstrated the potential of selectively transporting spins through chiral assemblies of supramolecular polymers, resulting in novel behaviors.[18–20] For instance, chiral supramolecular polymers have been utilized to enhance the efficiency of organic light-emitting diodes (OLEDs) by selectively injecting preferred spins, leading to increased light emission and efficiency without the need of an external magnetic field.[13] Another example involves the use of chiral porphyrin and triarylamine derivatives, which undergo supramolecular polymerization into helices of a specific handedness. These helices, when placed on an electrode surface, prevent the recombination of spins of the same type during water splitting, thereby reducing the formation of hydrogen peroxide.[21]

While many supramolecular polymers have been investigated, some possess the interesting ability to reversibly switch their chirality based on external parameters such as temperature,[18,22] pH,[22a,22b] light,[23] or solution aging time.[24] This property has been harnessed to develop chiroptical switches,[25] which are valuable tools for studying multifunctional electronic materials and exploring spin selectivity. In this work, we show spin polarization on supramolecular polymers with opposite handedness emerging from single enantiomers. The building blocks of the supramolecular polymers are based on a π-conjugated quinquethiophene segment coupled to rhodanine rings in both extremities (Figure 1a). The amide hydrogen-bonding units, necessary to guide the self-assembly process, are attached to the rhodanine rings by six-carbon alkyl linkers, and the chiral centers are provided by incorporating L or D-alanine methyl ester substituents (**QR-S** and **QR-R**, Figure 1a). The formation of the supramolecular polymers with opposite handedness was followed by UV-Vis and circular dichroism (CD) spectroscopies and their morphology by transmission electron microscopy (TEM). The spin polarization (P), which is defined as $P = \frac{(I_\alpha - I_\beta)}{(I_\alpha + I_\beta)}$ where I_α and I_β refer to the spin-specific experimental measurables (e.g., current, rate constant) for spin angular momentum aligned parallel and anti-parallel to the electron's velocity,[3,26]

was measured by scanning tunneling microscopy (STM) using scanning tunneling spectroscopy (STS) mode upon applying an external magnetic field. In the present study, the tunneling current ($I_{tunnel} \propto e^{-2\frac{\sqrt{2m\phi}}{\hbar}z}$, where z is the STM tip to surface distance and ϕ is the potential width) in STS was set at 8 nA, and the electrons tunnel through a very small gap of around 30 nm from the STM tip to the ITO surface.[26a]

We recently reported an interesting supramolecular system involving the inversion of chirality in a quinquethiophene-rhodanine derivative, diverging from a single enantiomer.[22] Our choice of this specific π-conjugated segment stems from its exceptional semiconducting properties in organic electronic devices.[27,28] We aim to delve into the domain of supramolecular polymers, exploring their potential applications in organic solar cells (OSCs) and organic field effect transistors (OFETs). Oligothiophenes are widely recognized as some of the most effective π-conjugated systems in organic electronics[29] and by coupling them to the electron-withdrawing rhodanine rings, these systems showed remarkable efficiency in diverse types of electronic devices.[27,28] Intriguingly, when we synthesized hydrogen-bonded analogues of the quinquethiophene-rhodanine system to form supramolecular polymers, slight variations in solvent mixtures and sample preparation resulted in the inversion of chirality within the supramolecular polymers in solution. Nevertheless, no chirality inversion was observed on thin film, making it difficult to explore spin polarization with the traditional techniques utilized.[3] In this work, we present new oligothiophene derivatives, **QR-L** and **QR-D** (Figure 1a), containing alanine substituents to introduce chiral centers. These new supramolecular polymers exhibit chirality inversion both in solution and thin films, making them excellent models for studying the CISS effect in supramolecular polymers with complex pathways. We expect that our findings make a significant impact on the development of chiral nanostructures, particularly in the realm of organic spintronics. These findings also hold potential for inspiring the scientific community to explore novel materials in the domains of asymmetric catalysis, chiroptical switches, and organic electronics, where precise management of electron spin is of utmost importance.

Results and discussion

The chiral building blocks, **QR-L** and **QR-D** (Figure 1a), have been synthesized following a previously described synthetic protocol.[22] The synthetic route included the coupling of derivative **1** (Scheme S1), that includes pending carboxylic acid groups, to L- or D-alanine methyl esters (Scheme S1) using hexafluorophosphate benzotriazole tetramethyl uranium (HBTU) as the coupling agent in basic conditions at room temperature. The final products were isolated by column chromatography and obtained in 64% and 74% yields for **QR-L** and **QR-D**, respectively. The building blocks were characterized by ^{1}H- and ^{13}C-NMR and high resolution mass spectrometry (see Section 2, ESI† for full characterization).

The self-assembly properties of **QR-L** and **QR-D** were followed by UV-Vis spectroscopy using initially dichloroethane (DCE) as the solvent (Figure 1b and 1c, black traces). In this case, the absorption spectra of **QR-L** and **QR-D** show a broad band with λ_{max} located at 499 nm that corresponds to the active chromophore, as reported for dilute solutions of the non-hydrogen-bonded analogues[27] and by our group in our previous work on hydrogen-bonded **QR** derivatives in the molecularly dissolved state.[22] In a next step we added a small percentage (10%) of methylcyclohexane (MCH) to promote aggregation (Figure 1b and 1c, blue and red traces). The samples were prepared either by heating and cooling at controlled rate (1°C/minute) or by sonication during 1h using an ice bath to avoid the increase of temperature. This way we ensured that we start from the molecularly dissolved state, and promote aggregation either by cooling down or stopping the sonication. In both cases, there was a broadening of the main absorption band and a red-shift to 550 nm and to 580 nm when the samples were heated/cooled or sonicated, respectively (Figure 1b and 1c, blue and red traces). These results already highlight the tendency of **QR-L** and **QR-D** to form aggregates in the DCE/MCH 9:1 mixture. Furthermore, the spectra displayed a new shoulder band with center at 670 nm (Figure 1b and 1c) that is attributed to the formation of J-type aggregates by hydrogen-bonding was observed. Similar results were found in analogue hydrogen-bonded **QR** systems[22] reported by us and other hydrogen-bonded π-conjugated derivatives.[30–33] Variable temperature (VT) UV-vis studies (Figure S1) revealed that the supramolecular polymers formed by **QR-L** and **QR-D** disassembled at high temperature (80 ºC), until reaching the

molecularly dissolved state, obtaining spectra similar to the one in DCE without any additional aggregation bands, and a blue shift of the main absorption band (Figure S1a and S1b).

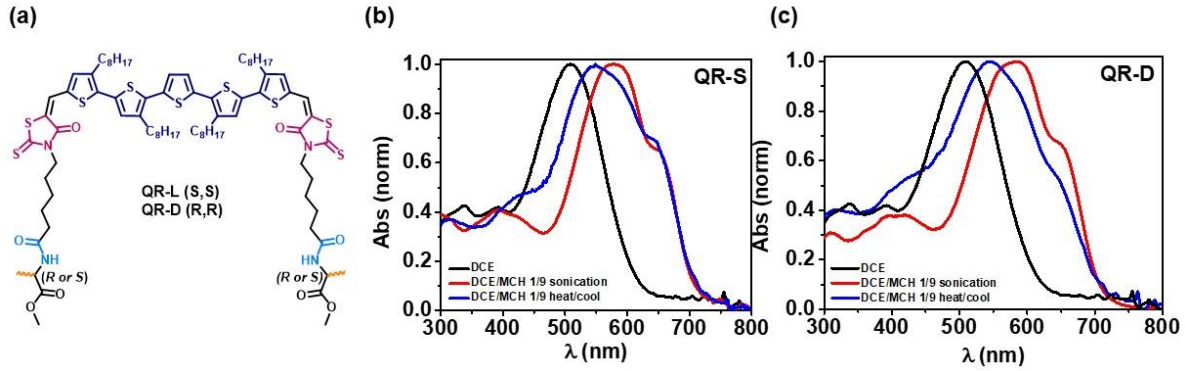

Figure 1. a) Chemical structure of **QR-L** and **QR-D**. Absorption spectra in DCE and DCE/MCH 1/9 solutions prepared by sonication or heat/cool at 1 °C/min of b) **QR-L** and c) **QR-D**. [**QR-L**] = [**QR-D**] = 20 μM.

We used circular dichroism (CD) spectroscopy to investigate the emergence of supramolecular chirality resulting from the aggregation of **QR-L** and **QR-D** in solution. In Figure 2, the CD spectra of **QR-L** and **QR-D** are depicted in both DCE and DCE/MCH 9:1 solution, prepared by heating/cooling (Figure 2a and 2b, blue trace) as well as sonication (Figure 2a and 2b, red trace). Interestingly, while the CD signal remains silent in DCE due to the absence of aggregates (black traces), the spectra in DCE/MCH solution at room temperature exhibit strong CD signals, indicating that the chirality of the assemblies is driven by supramolecular polymerization. Similarly, to the spectra in pure DCE, the CD signal was silent in the spectra of DCE/MCH solutions at high temperature (Figure S2a and S2b). Notably, the supramolecular structures formed by each single enantiomer prepared by the two different protocols display opposite chirality (Figure 2a and 2b). For instance, when the solution is sonicated, **QR-L** exhibits a positive signal at the J-aggregate wavelength, whereas when the solution is heated and cooled, it shows a negative signal (Figure 2a). **QR-D** follows a similar pattern, but with signals of opposite sign. Despite observing Cotton effect with the two different sample preparations, the signals are not mirror images, differing in intensity and wavelength. These findings suggest that the supramolecular polymerization mechanism and the arrangement of molecules undergo changes under

the different preparation protocols. Thus, even though the building blocks consist of single enantiomers, their secondary structure can be modified by external stimuli. In all cases, we discarded linear dichroism effects due to the almost insignificant signals measured (Figure S3).

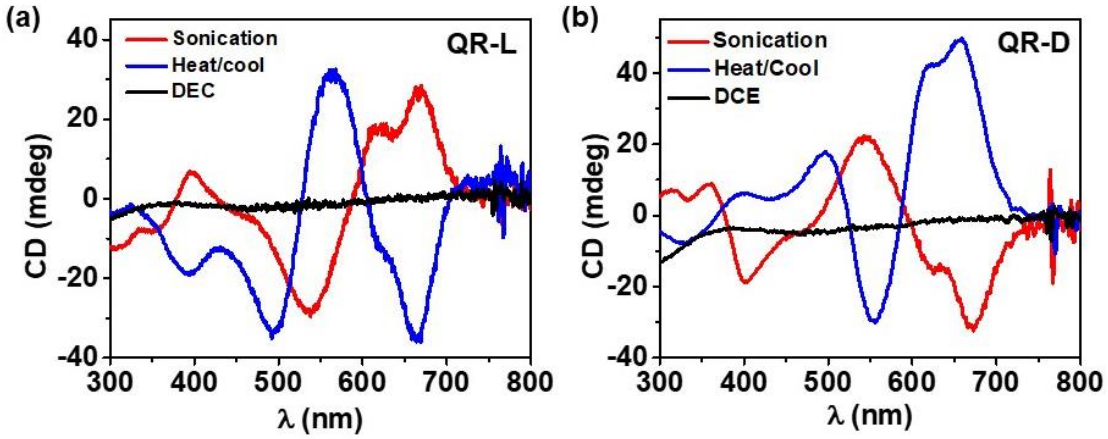

Figure 2. CD spectra in DCE and DCE/MCH 1/9 solutions prepared by sonication or heat/cool at 1 °C/min of (a) **QR-L** and (b) **QR-D**. [**QR-L**] = [**QR-D**] = 20 μM.

Similarly, to the results in solution, we also observed chirality inversion on thin films of **QR-L** and **QR-D** prepared by drop-casting DCE/MCH 9:1 solutions that were previously sonicated or heated/cooled (Figure 3a and 3b). In this case, the CD signals were much weaker than the ones in solution, but the sign of the signals was maintained with respect to the samples in solution. As in the case of solutions, the CD signals on thin film of each enantiomer prepared by different protocols are not mirror images. These results were very useful for the spin filtration studies by STM on STS mode (see below), since the presence of thin films is required to perform such measurements.

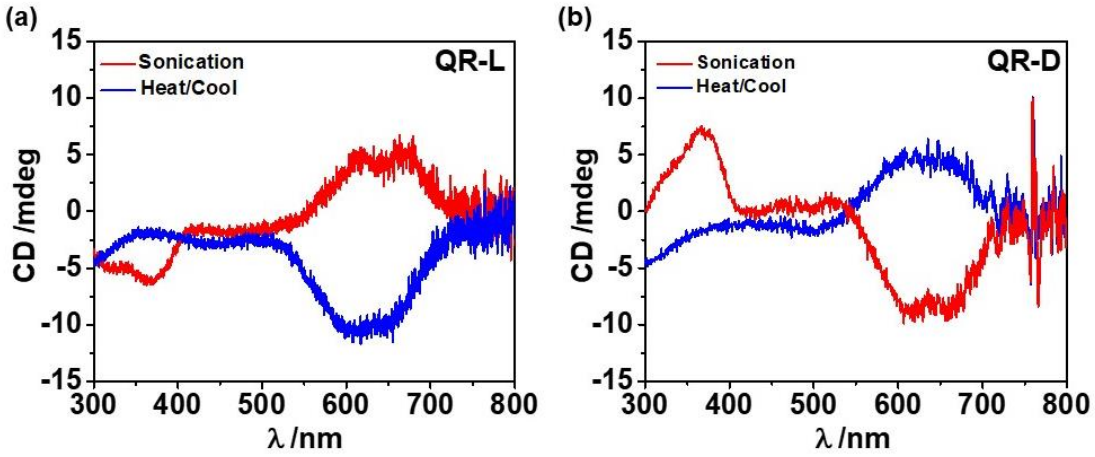

Figure 3. CD spectra on thin films prepared by drop-casting DCE/MCH 1/9 solution after sonication or heat/cooling of (a) **QR-L** and (b) **QR-D**. [**QR-L**] = [**QR-D**] = 20 μM.

The morphology of the supramolecular polymers formed by **QR-L** and **QR-D** was studied using transmission electron microscopy (TEM) on samples prepared by sonication or heating/cooling at controlled rate (Figure 4). In the case of the sonicated samples, **QR-L** and **QR-D** showed short-length twisted fibers that form larger aggregates of 50-100 nm in width (indicated with blue arrows in figure 4). When the samples were heated/cooled the morphology differed to the one of sonicated samples. In this case, much longer helical fibers were observed. The width of the observed helical fiber ranged from 80 to 150 nm once individual fibers assembled to form a secondary structure (red arrows in figure 4).

After the characterization of the chiral supramolecular polymers, we explored the spin-specific transport of **QR-L** and **QR-D** using STM on STS mode upon applying an external magnetic field (0.05 Tesla). STS is an extension of STM that provides information about the density of electrons in a sample as a function of their energy. The STM tip is used as a nanometer scale contact to obtain a plot of the current (I) as a function of the tip bias voltage (V).[26a,33a]

Thin films of **QR-L** and **QR-D** were prepared by drop-casting sonicated and heated/cooled solutions (Figure S4) in DCE/MCH 1:9 mixtures on indium tin oxide (ITO) substrates. The samples were measured at room temperature and ambient environment (See SI for details). An external magnetic field is placed below the sample holder and the STM tip trails over the sample surface to measure the *I-V* curve upon changing the direction of the magnetic field (up or down). This way, the electrons tunnel

from the substrate to the tip and vice-versa through the chiral assemblies. The electron's penetration strength depends on the supramolecular structure handedness and the magnetization direction, favouring a particular out of two different electron spin wave functions tunnelling into the film.

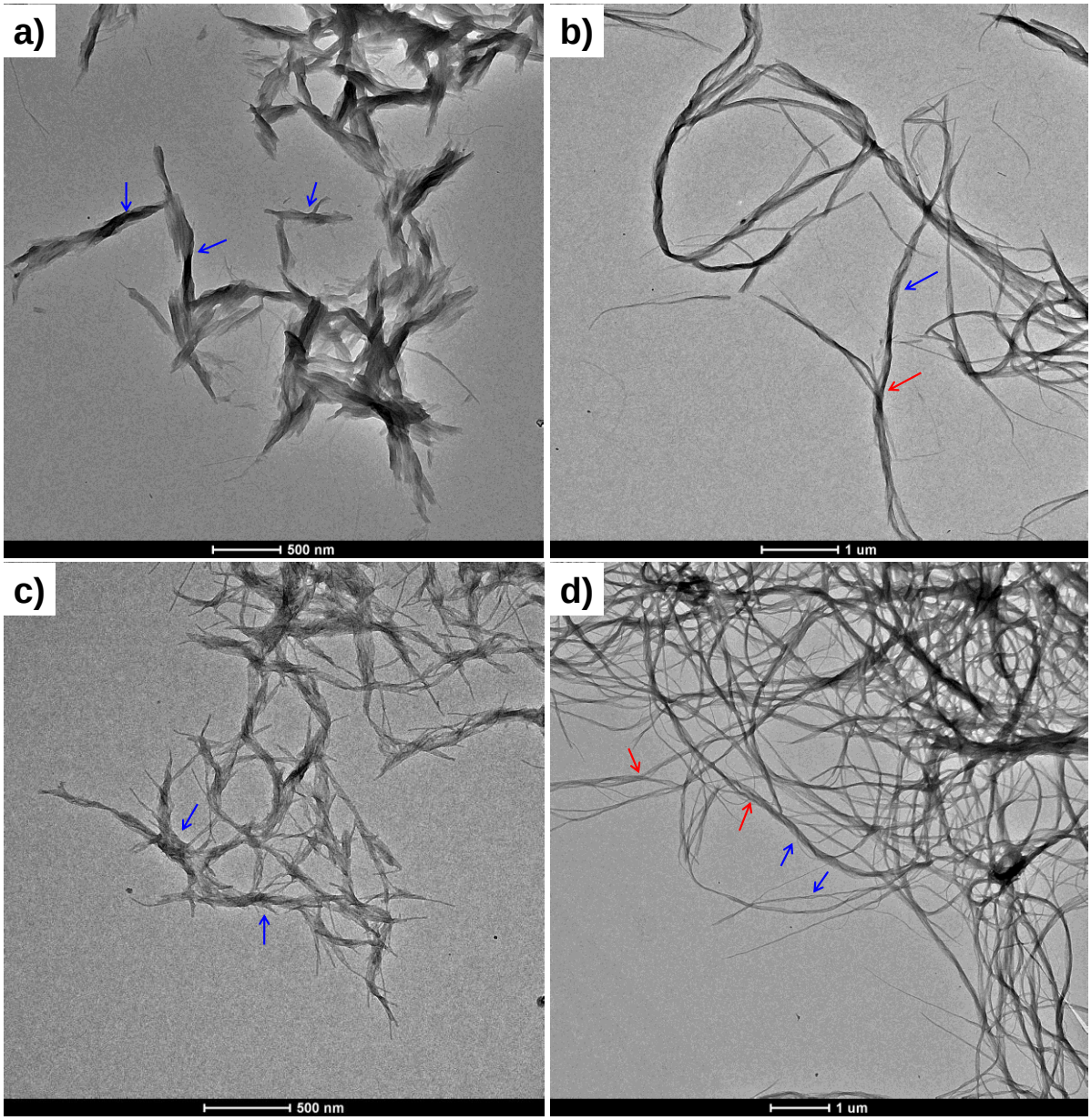

Figure 4. TEM images of **QR-L** prepared by (a) sonication and (b) thermal treatment, and **QR-D** prepared by (c) sonication and (d) thermal treatment. [**QR-L**] = [**QR-D**] = 20 μM in DCE/MCH 1/9. Blue arrows indicate twisted structures and red arrows indicate the formation of secondary structures.

Figure 5 illustrates the STS characteristics of **QR-L** and **QR-D** upon changing the direction of the magnetic field. Interestingly, a symmetric plateau centered at 0V was observed for both the **QR-L** and **QR-D** samples from sonicated solutions (Figure 5a and 5c), but for heated/cooled **QR-L** and **QR-D** samples (Figure 5b and 5d), significant offsets in the *I-V* curves were observed. The interactions of the two different chiral structures, **QR-L(D)** sonicated and **QR-L(D)** heated/cooled with the ITO substrate creates distinct contact potentials due to the CISS effect, which are reflected in the offsets in the *I-V* measurements.

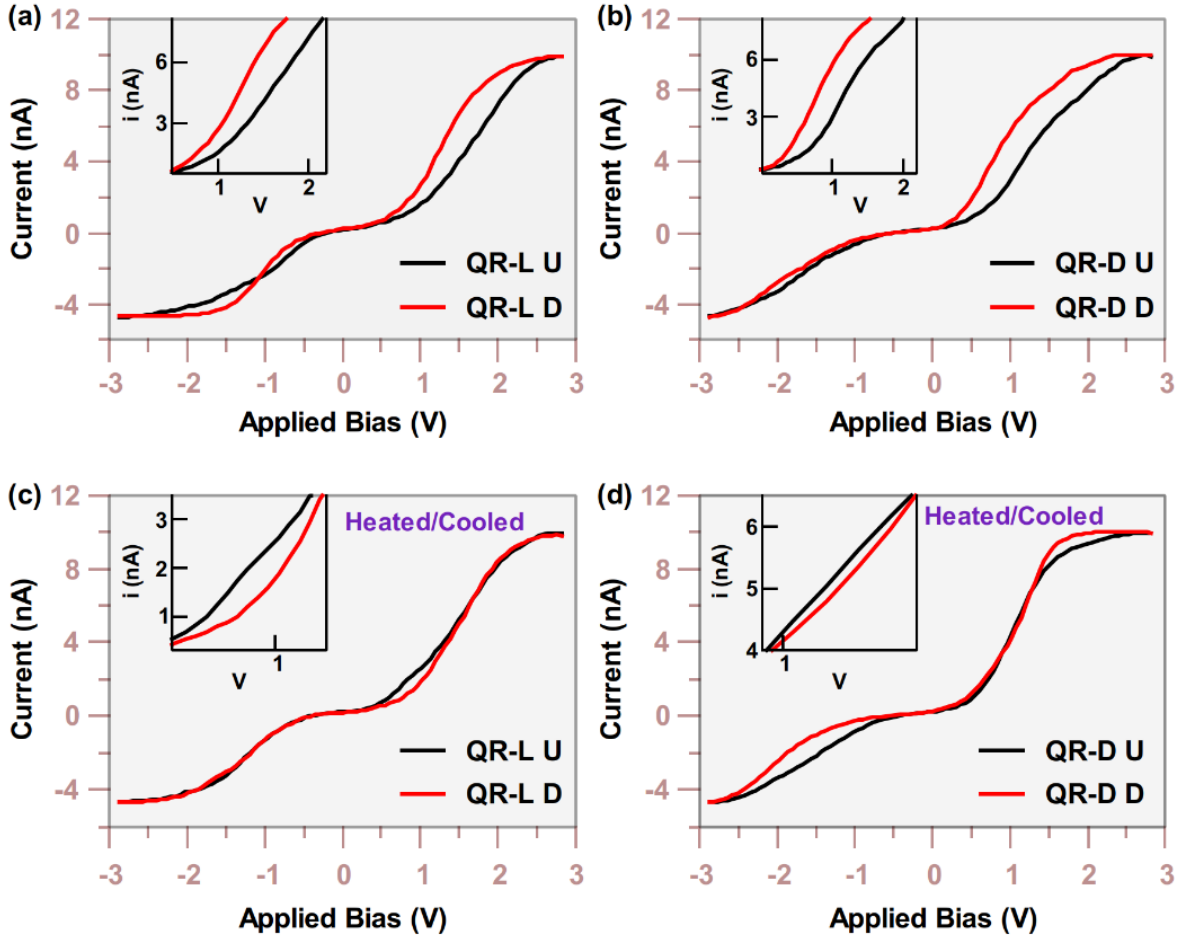

Figure 5: STS characteristics of **QR-L** and **QR-D** (with 8 nA tunneling current) for different preparation protocols with "up (U)" and "down (D)" magnetic field directions with respect to the ITO surface. (a) **QR-L** film from sonicated solutions. (b) **QR-D** films from sonicated solutions. (c) **QR-L** from heated/cooled solutions. (d) **QR-D** films from heated/cooled solutions.

As previously shown in figure 3, the CD spectra of **QR-L** and **QR-D** on thin films cast from solutions prepared by different protocols showed chirality inversion. Therefore, we anticipated that the spin polarization would be reversed as well. This is shown in figure 6, where the percentages of spin polarization for **QR-L** films cast from sonicated solutions and heated/cooled samples at 1V applied bias are of -25% and +17%, respectively (Figure 6a and c). Regarding **QR-D**, the percentages of spin polarization at 1V bias for films cast from sonicated solutions and heated/cooled ones were of -30% and +3%, respectively (Figure 6b and d). The maximum spin polarization recorded for each sample was of -30% and -42% for films prepared from sonicated solutions of **QR-D** and **QR-L** (Figure 6a and 6b), respectively and of +25% and +3% for films prepared by heated/cooled solutions of **QR-L** and **QR-D**, respectively (Figure 6c and 6d).

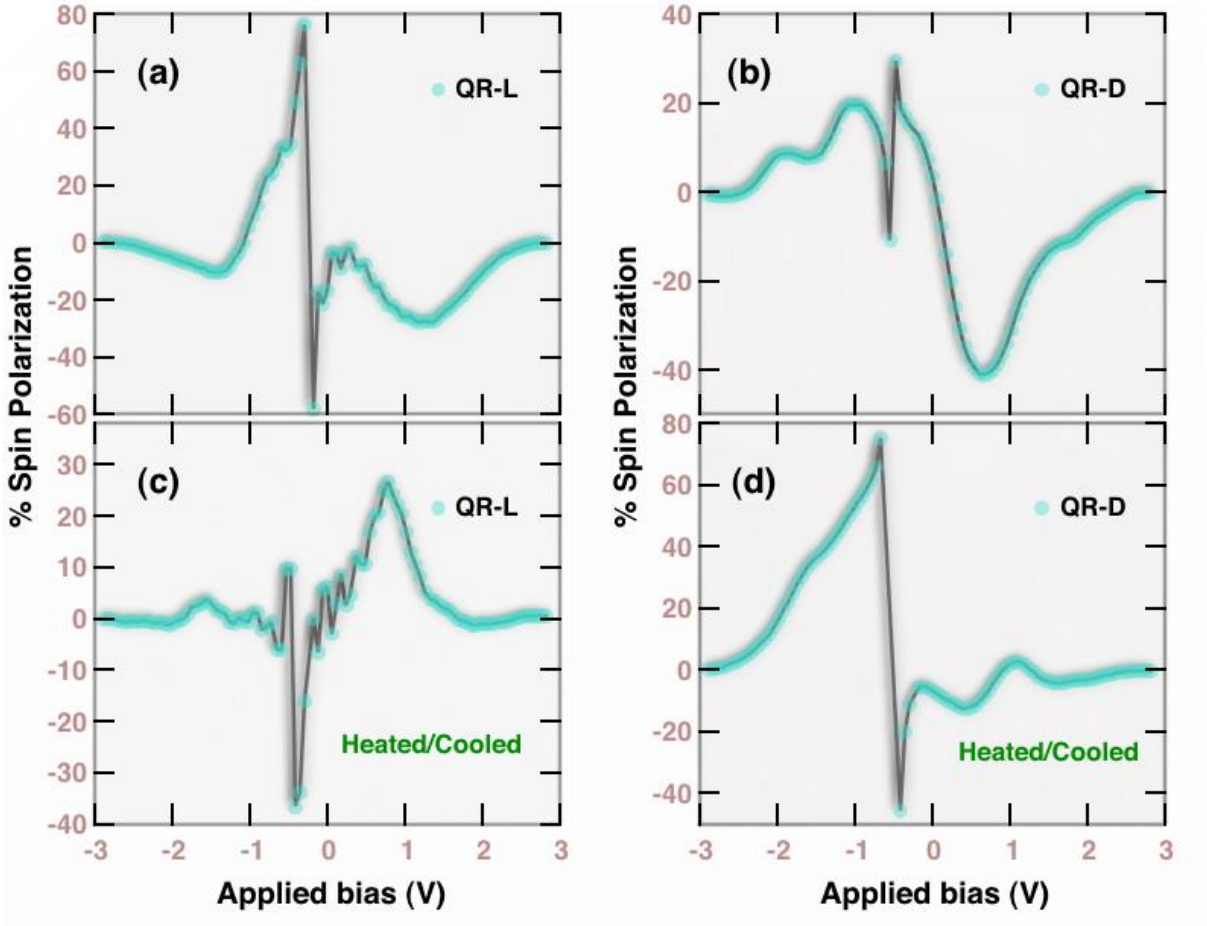

Figure 6. Spin filtration characteristics of **QR-L** and **QR-D** molecules for different preparation protocols. (a) **QR-L** film from sonicated solutions. (b) **QR-D** films from sonicated solutions. (c) **QR-L** from heated/cooled solutions. (d) **QR-D** films from heated/cooled solutions.

The TEM images of **QR-L** and **QR-D** shown in figure 4 reflect morphological differences between the two different sample preparations. As previously described, the samples prepared from sonicated solutions show shorter but wider aggregates of twisted fibers than the samples prepared by thermal treatment, resulting in better adsorption as well as high density of fibers onto the ITO substrates. Thus, these samples exhibited higher spin filtration percentages (Figure 6a and 6b) than the samples prepared by thermal treatment (Figure 6b and 6d). In contrast, the structures formed by controlled heating/cooling are twisted fibers with higher aspect-ratio than the structures formed by sonication. We can think of these supramolecular structures as long helical tubes with finite radius and pitch.[10] The confinement potential restricts the charge particle motion to the proximity of the helix curve. Assuming that the shape of the potential does not vary along the curve and that the potential is spherically symmetric, the strong confinement being equivalent to the tube having a radius close to zero. It is also known that the spin polarization increases with the length of the supramolecular structures with a roughly linear correlation[7,10]. There have been numerous reports of organic compounds having active groups, including carboxylic acid and ester, forming self-assembled monolayers (SAM) on ITO[12-16] substrates. Due to the shorter length in the supramolecular structures of sonicated **QR-L** and **QR-D** molecules, the arrangement of SAMs is such that the residence time of the electrons in the chiral system is larger with high density spins accumulation, making even a small spin orbit coupling very effective, and subsequently, higher spin polarization comparing to the thermally treated **QR-L** and **QR-D** supramolecular structures. These results confirm that **QR-L** and **QR-D** show different spin selectivity for supramolecular polymers obtained under different conditions. It is important to remark that the spin filtration measurements are done on supramolecular structures physiosorbed onto ITO substrates, having no control over the orientation of the supramolecular polymers. While this technique has the advantage of preparing the samples in an easy manner, our future directions are focused on modifying

the building blocks so they can be grafted to surfaces and electrodes in order to obtain SAMs with precise structure.

Conclusions

In conclusion, our findings demonstrate the remarkable capability to manipulate and quantify spin specificity in chiral supramolecular polymers derived from single enantiomers, showcasing opposing handedness. Through the synthesis of two enantiomers of quinquethiophene-rhodanine derivatives, we successfully generated supramolecular polymers facilitated by hydrogen-bonding interactions. By varying the sample preparation methods, distinct chiral supramolecular structures were obtained, each exhibiting different spin filtration percentages, as revealed through STM conducted in STS mode. Interestingly, the supramolecular polymers prepared via sonication of solutions exhibited higher spin filtration rates. Further investigation will be performed to elucidate the underlying factors contributing to the properties of these specific structures. While film deposition via drop-casting from solution offers convenience in measurement, we hope to enhance our results by precisely controlling the growth of the supramolecular structures on substrates. Through this study, we aim to highlight the potential of chiroptical switching in supramolecular polymers in the field of spin selectivity and functional spintronic devices.

Authors contribution

AMG synthesized the molecules, KH performed UV and CD spectroscopy, AK performed the STM on STS mode measurements. SM and ARC conceived the project and supervised the work. All the authors contributed to the discussion and the writing of the manuscript.

Conflict of interest

The authors declare no conflict of interest

Funding

University of Strasbourg Institute for Advanced Science (USIAS 2020). Initiative d'Excellence.

Acknowledgments

This work has benefitted from support provided by the University of Strasbourg Institute for Advanced Study (USIAS) for a Fellowship, within the French national programme "Investment for the future" (IdEx-Unistra).

AMG, KH and ARC thank the characterization (CarMac) and microscopy (PLAMICS) platforms of Institute Charles Sadron.

References

[1] S. Paul, A.S. Kiryutin, J. Guo, K.L. Ivanov, J. Matysik, A.V. Yurkovskaya, and X. Wang, "Magnetic field effect in natural cryptochrome explored with model compound," Sci Rep **7**(1), 1–10 (2017).
[2] C. Yang, Y. Li, S. Zhou, Y. Guo, C. Jia, Z. Liu, K.N. Houk, Y. Dubi, and X. Guo, "Real-time monitoring of reaction stereochemistry through single-molecule observations of chirality-induced spin selectivity," Nat. Chem., 1–8 (2023).
[3] R. Naaman, and D.H. Waldeck, "Chiral-Induced Spin Selectivity Effect," The Journal of Physical Chemistry Letters **3**(16), 2178–2187 (2012).
[4] K. Ray, S.P. Ananthavel, D.H. Waldeck, and R. Naaman, "Asymmetric Scattering of Polarized Electrons by Organized Organic Films of Chiral Molecules," Science **283**(5403), 814–816 (1999).
[5] S. Mishra, A.K. Mondal, S. Pal, T.K. Das, E.Z.B. Smolinsky, G. Siligardi, and R. Naaman, "Length-Dependent Electron Spin Polarization in Oligopeptides and DNA," J. Phys. Chem. C **124**(19), 10776–10782 (2020).
[6] M. Kettner, B. Göhler, H. Zacharias, D. Mishra, V. Kiran, R. Naaman, D.H. Waldeck, S. Sęk, J. Pawłowski, and J. Juhaniewicz, "Spin Filtering in Electron Transport Through Chiral Oligopeptides," J. Phys. Chem. C **119**(26), 14542–14547 (2015).
[7] I. Carmeli, V. Skakalova, R. Naaman, and Z. Vager, "Magnetization of Chiral Monolayers of Polypeptide: A Possible Source of Magnetism in Some Biological Membranes," Angewandte Chemie **114**(5), 787–790 (2002).
[8] S.G. Ray, S.S. Daube, G. Leitus, Z. Vager, and R. Naaman, "Chirality-Induced Spin-Selective Properties of Self-Assembled Monolayers of DNA on Gold," Phys. Rev. Lett. **96**(3), 036101 (2006).
[9] B. Göhler, V. Hamelbeck, T.Z. Markus, M. Kettner, G.F. Hanne, Z. Vager, R. Naaman, and H. Zacharias, "Spin Selectivity in Electron Transmission Through Self-Assembled Monolayers of Double-Stranded DNA," Science **331**(6019), 894–897 (2011).
[10] F. Tassinari, D.R. Jayarathna, N. Kantor-Uriel, K.L. Davis, V. Varade, C. Achim, and R. Naaman, "Chirality Dependent Charge Transfer Rate in Oligopeptides," Advanced Materials **30**(21), 1706423 (2018).
[11] R. Torres-Cavanillas, G. Escorcia-Ariza, I. Brotons-Alcázar, R. Sanchis-Gual, P.C. Mondal, L.E. Rosaleny, S. Giménez-Santamarina, M. Sessolo, M. Galbiati, S. Tatay, A. Gaita-Ariño, A. Forment-Aliaga, and S. Cardona-Serra, "Reinforced Room-Temperature Spin Filtering in Chiral Paramagnetic Metallopeptides," J. Am. Chem. Soc. **142**(41), 17572–17580 (2020).
[12] H. Lu, J. Wang, C. Xiao, X. Pan, X. Chen, R. Brunecky, J.J. Berry, K. Zhu, M.C. Beard, and Z.V. Vardeny, "Spin-dependent charge transport through 2D chiral hybrid lead-iodide perovskites," Science Advances **5**(12), eaay0571 (2019).
[13] P.C. Mondal, N. Kantor-Uriel, S.P. Mathew, F. Tassinari, C. Fontanesi, and R. Naaman, "Chiral Conductive Polymers as Spin Filters," Advanced Materials **27**(11), 1924–1927 (2015).
[14] S. Mishra, A.K. Mondal, E.Z.B. Smolinsky, R. Naaman, K. Maeda, T. Nishimura, T. Taniguchi, T. Yoshida, K. Takayama, and E. Yashima, "Spin Filtering Along Chiral Polymers," Angew Chem Int Ed Engl **59**(34), 14671–14676 (2020).

[15] U. Huizi-Rayo, J. Gutierrez, J.M. Seco, V. Mujica, I. Diez-Perez, J.M. Ugalde, A. Tercjak, J. Cepeda, and E. San Sebastian, "An Ideal Spin Filter: Long-Range, High-Spin Selectivity in Chiral Helicoidal 3-Dimensional Metal Organic Frameworks," Nano Lett. **20**(12), 8476–8482 (2020).
[16] M. Suda, Y. Thathong, V. Promarak, H. Kojima, M. Nakamura, T. Shiraogawa, M. Ehara, and H.M. Yamamoto, "Light-driven molecular switch for reconfigurable spin filters," Nature Communications **10**(1), 2455 (2019).
[17] T. Aida, E.W. Meijer, and S.I. Stupp, "Functional supramolecular polymers," Science **335**(6070), 813–817 (2012).
[18] C. Kulkarni, A.K. Mondal, T.K. Das, G. Grinbom, F. Tassinari, M.F.J. Mabesoone, E.W. Meijer, and R. Naaman, "Highly Efficient and Tunable Filtering of Electrons' Spin by Supramolecular Chirality of Nanofiber-Based Materials," Advanced Materials **32**(7), 1904965 (2020).
[19] A.K. Mondal, M.D. Preuss, M.L. Ślęczkowski, T.K. Das, G. Vantomme, E.W. Meijer, and R. Naaman, "Spin Filtering in Supramolecular Polymers Assembled from Achiral Monomers Mediated by Chiral Solvents," J. Am. Chem. Soc., jacs.1c02983 (2021).
[20] A.T. Rösch, Q. Zhu, J. Robben, F. Tassinari, S.C.J. Meskers, R. Naaman, A.R.A. Palmans, and E.W. Meijer, "Helicity Control in the Aggregation of Achiral Squaraine Dyes in Solution and Thin Films," Chemistry **27**(1), 298–306 (2021).
[21] W. Mtangi, F. Tassinari, K. Vankayala, A. Vargas Jentzsch, B. Adelizzi, A.R.A. Palmans, C. Fontanesi, E.W. Meijer, and R. Naaman, "Control of Electrons' Spin Eliminates Hydrogen Peroxide Formation During Water Splitting," J. Am. Chem. Soc. **139**(7), 2794–2798 (2017).
[22] A.M. Garcia, and A. Ruiz-Carretero, "Chirality inversion in hydrogen-bonded rhodanine–oligothiophene derivatives by solvent and temperature," Chem. Commun. **58**(4), 529–532 (2022).
[22a] F. Ceccacci, G. Mancini, A. Sferrazza, and C. Villani, "pH variation as the switch for chiral recognition in a biomembrane model," J Am Chem Soc 127(40), 13762–13763 (2005).

[22b] A. Kousar, J. Liu, N. Mehwish, F. Wang, A.Y. Dang-i, and C. Feng, "pH-Regulated supramolecular chirality of phenylalanine-based hydrogels," Mater Today Chem 11, 217–224 (2019).

[23] P. Duan, Y. Li, L. Li, J. Deng, and M. Liu, "Multiresponsive Chiroptical Switch of an Azobenzene-Containing Lipid: Solvent, Temperature, and Photoregulated Supramolecular Chirality," J. Phys. Chem. B **115**(13), 3322–3329 (2011).
[24] A. Lohr, M. Lysetska, and F. Würthner, "Supramolecular Stereomutation in Kinetic and Thermodynamic Self-Assembly of Helical Merocyanine Dye Nanorods," Angew. Chem. Int. Ed. **44**(32), 5071–5074 (2005).
[25] L. Zhang, H.-X. Wang, S. Li, and M. Liu, "Supramolecular chiroptical switches," Chemical Society Reviews **49**(24), 9095–9120 (2020).
[26] M. Julliere, "Tunneling between ferromagnetic films," Physics Letters A **54**(3), 225–226 (1975).
[26a] C. Pal, and S. Majumder, "Manipulating electron-spin polarization using cysteine-DNA chiral conjugates," Journal of Chemical Physics **156** (16), (2022).

[27] B. Kan, M. Li, Q. Zhang, F. Liu, X. Wan, Y. Wang, W. Ni, G. Long, X. Yang, H. Feng, Y. Zuo, M. Zhang, F. Huang, Y. Cao, T.P. Russell, and Y. Chen, "A Series of Simple Oligomer-like Small Molecules Based on Oligothiophenes for Solution-Processed Solar Cells with High Efficiency," Journal of the American Chemical Society **137**(11), 3886–3893 (2015).
[28] Q. Zhang, B. Kan, F. Liu, G. Long, X. Wan, X. Chen, Y. Zuo, W. Ni, H. Zhang, M. Li, Z. Hu, F. Huang, Y. Cao, Z. Liang, M. Zhang, T.P. Russell, and Y. Chen, "Small-molecule solar cells with efficiency over 9%," Nature Photon **9**(1), 35–41 (2015).
[29] G. Barbarella, M. Melucci, and G. Sotgiu, "The versatile thiophene: an overview of recent research on thiophene-based materials," Advanced Materials **17**(13), 1581–1593 (2005).
[30] S. Ghosh, S. Cherumukkil, C.H. Suresh, and A. Ajayaghosh, "A Supramolecular Nanocomposite as a Near-Infrared-Transmitting Optical Filter for Security and Forensic Applications," Advanced Materials **29**(46), 1703783 (2017).
[31] S. Militzer, T.M.P. Tran, P.J. Mésini, and A. Ruiz-Carretero, "Tuning the Optical and Self-Assembly Properties of Diketopyrrolopyrrole Semicarbazone Derivatives through Hydrogen Bonding," ChemNanoMat **4**(8), 790–795 (2018).

[32] S. Militzer, N. Nishimura, N.R. Ávila-Rovelo, W. Matsuda, D. Schwaller, P.J. Mésini, S. Seki, and A. Ruiz-Carretero, "Impact of Chirality on Hydrogen-Bonded Supramolecular Assemblies and Photoconductivity of Diketopyrrolopyrrole Derivatives," Chemistry - A European Journal **26**(44), 9998–10004 (2020).
[33] N.R. Ávila-Rovelo, G. Martinez, W. Matsuda, S. Sinn, P. Lévêque, D. Schwaller, P. Mésini, S. Seki, and A. Ruiz-Carretero, "Hydrogen-Bonded Organic Semiconductors with Long Charge Carrier Lifetimes," J. Phys. Chem. C **126**(26), 10932–10939 (2022).
[33b] R.M. Feenstra, Scanning Tunneling Spectroscopy (n.d.).